

See discussions, stats, and author profiles for this publication at: <http://www.researchgate.net/publication/266149886>

# THORACOLUMBAR INTRADURAL DISC HERNIATION IN EIGHT DOGS: CLINICAL, LOW- FIELD MAGNETIC RESONANCE IMAGING, AND COMPUTED TOMOGRAPHIC MYELOGRAPHY FINDINGS

ARTICLE *in* VETERINARY RADIOLOGY & AMP ULTRASOUND · SEPTEMBER 2014

Impact Factor: 1.26 · DOI: 10.1111/vru.12213

---

DOWNLOADS

19

---

VIEWS

33

7 AUTHORS, INCLUDING:



**Tsuyoshi Ozawa**

Japan Animal Referral Medical Center

13 PUBLICATIONS 47 CITATIONS

SEE PROFILE

# THORACOLUMBAR INTRADURAL DISC HERNIATION IN EIGHT DOGS: CLINICAL, LOW-FIELD MAGNETIC RESONANCE IMAGING, AND COMPUTED TOMOGRAPHIC MYELOGRAPHY FINDINGS

SHINJI TAMURA, SHOKO DOI, YUMIKO TAMURA, KUNIAKI TAKAHASHI, HIROKAZU ENOMOTO, TSUYOSHI OZAWA, KAZUYUKI UCHIDA

Intradural disc herniation is a rarely reported cause of neurologic deficits in dogs and few published studies have described comparative imaging characteristics. The purpose of this retrospective cross sectional study was to describe clinical and imaging findings in a group of dogs with confirmed thoracolumbar intradural disc herniation. Included dogs were referred to one of four clinics, had acute mono/paraparesis or paraplegia, had low field magnetic resonance imaging (MRI) and/or computed tomographic myelography, and were diagnosed with thoracolumbar intradural disc herniation during surgery. Eight dogs met inclusion criteria. The prevalence of thoracolumbar intradural disc herniation amongst the total population of dogs that developed a thoracolumbar intervertebral disc herniation and that were treated with a surgical procedure was 0.5%. Five dogs were examined using low-field MRI. Lesions that were suspected to be intervertebral disc herniations were observed; however, there were no specific findings indicating that the nucleus pulposus had penetrated into the subarachnoid space or into the spinal cord parenchyma. Thus, the dogs were misdiagnosed as having a conventional intervertebral disc herniation. An intradural extramedullary disc herniation (three cases) or intramedullary disc herniation (two cases) was confirmed during surgery. By using computed tomographic myelography (CTM) for the remaining three dogs, an intradural extramedullary mass surrounded by an accumulation of contrast medium was observed and confirmed during surgery. Findings from this small sample of eight dogs indicated that CTM may be more sensitive for diagnosing canine thoracolumbar intradural disc herniation than low-field MRI. © 2014 American College of Veterinary Radiology.

**Key words:** CT myelography, dog, intradural disc herniation, MRI.

## Introduction

**I**INTRADURAL DISC HERNIATION WITH an extruded nucleus pulposus penetrating the dura mater is a rarely reported cause of neurologic deficits in dogs.<sup>1-8</sup> Extruded nuclei pulposi may be present in the subarachnoid space (intradural extramedullary disc herniation)<sup>1,4,7</sup> or in the spinal cord parenchyma (intramedullary disc herniation).<sup>2,3,5,6,8</sup> Almost all cases in past reports had suffered a traumatic event following physical activity, such as running, jumping, and racing,<sup>1,3-6,8</sup> although one case was reported as having a spontaneous intradural disc herniation.<sup>7</sup> Reports describ-

ing the prevalence of intradural disc herniation in dogs are currently lacking.

Preoperative diagnosis of intradural disc herniation is often challenging in both dogs and humans because of variable clinical presentation and radiological appearance.<sup>9</sup> In almost all human cases described in the literature, a diagnosis of an intradural disc herniation could be identified only during surgery.<sup>10</sup> Little information is available regarding a preoperative diagnostic approach for detecting canine intradural disc herniation. A “golf tee sign” suggests an intradural extramedullary lesion, as reported from observations of myelographic images.<sup>1,4</sup> Based on computed tomographic myelography (CTM), an intradural filling defect above the intervertebral disc space has previously been reported in two dogs.<sup>1,7</sup> The use of CTM proved to be valuable in demonstrating the presence of fragmented disc material in the dilated subarachnoid space in a dog discussed in one previous report.<sup>7</sup> A postmyelogram contrast leakage, suggesting a dural tear, has also been reported based on myelographic and CTM images.<sup>1,5,6</sup> However, it is important to note that the absence of a contrast medium

---

From the Tamura Animal Clinic, 7-16 Yoshimien, Saeki-ku, Hiroshima, 731-5132, Japan (Tamura, Doi, Tamura); Hidamari Animal Clinic, 3-11 Koran Gifu, Gifu, 500-8891, Japan (Takahashi); Enomoto Animal Hospital, Sapporo, Japan (Enomoto); Ozawa Animal Hospital, Uji, Japan (Ozawa); Department of Veterinary Pathology, Graduate School of Agricultural and Life Sciences, The University of Tokyo, Bunkyo-ku, Tokyo, Japan (Uchida).

Funding Sources: None

Address correspondence and reprint requests to Shinji Tamura, at the above address. E-mail: cqx03426@ms8.megaegg.ne.jp

Received January 30, 2014; accepted for publication June 22, 2014.  
doi: 10.1111/vru.12213

---

*Vet Radiol Ultrasound*, Vol. 56, No. 2, 2015, pp 160–167.

leakage does not preclude the possibility of a penetrating intradural or intramedullary disc herniation.<sup>7</sup> Intramedullary contrast medium was observed upon CTM in a case of canine intramedullary intradural disc herniation.<sup>8</sup> Furthermore, a canine intradural disc herniation case has been examined with high-field MRI; however, only a spinal cord abnormality was indicated, so that diagnosis necessitated exploratory surgery and a biopsy.<sup>2</sup> Additionally, as for other animals, only a feline case was diagnosed as having an intradural disc herniation, using radiography and high-field MRI findings.<sup>11</sup> Consequently, this case was rare, as a hemorrhage along the intramedullary tract of a very small, mineralized, and migrated nucleus pulposus was found by using T2\* weighted images (T2\*WI). The purpose of this retrospective cross sectional study was to describe the clinical, low field MRI and computed tomographic myelography characteristics in a group of dogs that were diagnosed with a thoracolumbar intradural disc herniation during surgery.

### Materials and Methods

Medical records of four different clinics were reviewed to identify dogs that had low field MRI or computed tomographic myelography (CTM) and that had a confirmed diagnosis of thoracolumbar intradural disc herniation. Case selection was not restricted by breed, age, degree, or onset of clinical signs. Records were also reviewed to identify all dogs with confirmed thoracolumbar disc herniation. For included dogs with a confirmed diagnosis of thoracolumbar intradural disc herniation, low field MRI, and CTM findings were recorded based on a consensus opinion of four readers. Evaluators first performed independent assessments and were allowed to adjust image displays or use multiplanar reformatting at will. Surgical findings were recorded based on medical record entries.

### Results

A total of 1605 dogs had a thoracolumbar intervertebral disc herniation and were then treated using a surgical procedure during the observation period (831 dogs, 2001–2013 in Tamura Animal Clinic; 72 dogs, 2008–2013 in Hidamari Animal Hospital; 533 dogs, 2008–2013 in Enomoto Animal Hospital; and 169 dogs, 2008–2013 in Ozawa Animal Hospital). Among them, eight cases were confirmed to have thoracolumbar intradural disc herniation during surgery. Details for each of the cases are summarized in Appendix 1. The cases included five Miniature Dachshunds, one Maltese, one Chihuahua, and one mixed small breed. All cases had an acute onset and did not suffer a traumatic event following physical activity, such as running, jumping, or racing, before onset. Six of the eight cases had back pain

or paraparesis in the past, prior to the presenting event. The prevalence of thoracolumbar intradural disc herniation within the total population of dogs that developed a thoracolumbar intervertebral disc herniation and were treated with a surgical procedure was 0.498%.

Low field MRI images of the thoracolumbar spine had been acquired for cases 1–5 using two different scanners (Airis II Confort, 0.3T, Hitachi Medical Corporation, Tokyo, Japan for cases 1, 2, 4, and 5; and Airis Mate, 0.2T, Hitachi Medical Corporation, Tokyo, Japan for case 3). A knee coil and general anesthesia were used for all cases. Pulse sequences and technique settings were as follows: T2-weighted sagittal (T2W-FSE: repetition time (TR), 4000 ms; echo time (TE), 125 ms; number of acquisitions (NEX), 4; slice thickness, 3 mm; interslice gap, 0 mm; field of view (FOV), 300 mm; matrix acquisition, 512 × 512; and voxel size, 1.04 × 1.34 × 3 mm) and transverse (T2W-FSE: TR, 4000 ms; TE, 125 ms; NEX, 6; slice thickness, 3 mm; interslice gap, 0.5 mm; FOV, 160 mm; matrix dimensions, 256 × 256; and voxel size, 0.625 × 0.8 × 3 mm) images were obtained for cases 1, 2, 4, and 5. Additional T2-weighted dorsal images (T2W-FSE: TR, 4000 ms; TE, 125 ms; NEX, 6; slice thickness, 3 mm; interslice gap, 0.5 mm; FOV, 160 mm; matrix dimensions, 256 × 256; and voxel size, 0.625 × 0.8 × 3 mm) were obtained for case 4. Additional T1-weighted transverse images (T1W-SE: TR, 450 ms; TE, 20 ms; NEX, 4; slice thickness, 3 mm; interslice gap, 0.5 mm; FOV, 160 mm; matrix dimensions, 256 × 256; and voxel size, 0.625 × 0.889 × 3 mm) were obtained for case 1. T2-weighted sagittal (T2W-FSE: TR, 3200 ms; TE, 120 ms; NEX, 12; slice thickness, 2.5 mm; interslice gap, 1.5 mm; FOV, 250 mm; matrix dimensions, 256 × 224; and voxel size, 0.977 × 1.116 × 2.5 mm) and transverse (T2W-FSE: TR, 3000 ms; TE, 120 ms; NEX, 14; slice thickness, 5.5 mm; interslice gap, 0 mm; FOV, 130 mm; matrix dimensions, 256 × 256; and voxel size, 0.508 × 0.508 × 5.5 mm) images, as well as pre- and post-contrast T1-weighted sagittal (T1W-SE: TR, 300 ms; TE, 23.8 ms; NEX, 8; slice thickness, 2.5 mm; interslice gap, 1.5 mm; FOV, 250 mm; matrix dimensions, 256 × 224; and voxel size, 0.977 × 1.116 × 2.5 mm) and transverse (T1W-SE: TR, 300 ms; TE, 17.7 ms; NEX, 8; slice thickness, 5.5 mm; interslice gap, 1.5 mm; FOV, 130 mm; matrix dimensions, 288 × 224; and voxel size, 0.451 × 0.580 × 5.5 mm) images, were obtained for case 3. Postcontrast MRI images had been acquired for case 3 immediately following manual, intravenous administration of meglumine gadopentetate (Magnevist; Bayer, Tokyo, Japan; 0.15 mmol/kg body weight).

Computed tomographic myelography (CTM) images of the thoracic to sacral spine had been acquired under general anesthesia for cases 6–8 using two different scanners (ROBUSTO Ei, Hitachi Medical Corporation, Tokyo, Japan for cases 6–7; and Asteion 4, Toshiba, Tokyo, Japan for case 8). Technique settings for cases 6–7 were as follows:

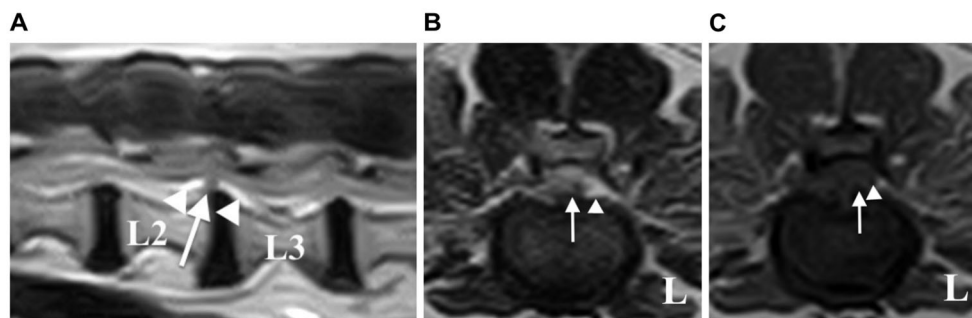


FIG. 1. Low field MRI scans for case 1. (A) T2-weighted left-sided parasagittal image. A hypointense mass (arrow) and hyperintense lesions indicating fluid (arrow heads) are evident at the level of the L2–3 intervertebral disc space. (B) T2-weighted transverse image. A hypointense mass (arrow) is present on the left side, ventral to the spinal cord. A hyperintense lesion (arrowhead), indicating fluid accumulation, is observed. (C) T1-weighted transverse image. The mass is hypointense (arrow), and a lesion indicating fluid with T2WI is hypointense (arrowhead).

section collimation thickness, 1.25 mm; image reconstruction interval, 1.25 mm; pitch, 3.0 mm; tube rotation time, 1.0 s, 175 mA, and 120 kVp; image field of view, 105 mm; matrix dimensions  $512 \times 512$ ; reconstruction algorithm, bone; window width, 2500; window level, +400; multiplanar reformatting was used; voxel size,  $0.31 \times 0.31 \times 2.5$  mm. Technique settings for case 8 were as follows: section collimation thickness, 2.0 mm; image reconstruction interval, 2.0 mm; pitch, 3.5 mm; tube rotation time, 0.75 s, 100 mA, and 120 kVp; image field of view, 320 mm; matrix dimensions,  $512 \times 512$ ; reconstruction algorithm. Computed tomographic myelography images for cases 6–8 were acquired immediately following subarachnoid administration of iohexol at L5–6 (Omnipaque 240, Daiichi Sankyo, Tokyo, Japan, iodine concentration 240 mg/ml, 0.45 ml/kg body weight for cases 6–7; Omnipaque 300, Daiichi Sankyo, Tokyo, Japan, iodine concentration 300 mg/ml, 0.5 ml/kg body weight for case 8).

MRI findings were initially recorded by one reader (ST for cases 1, 2, 4, 5; and KT for case 3). The final interpretation of the MRI scans was based on the consensus opinion of four authors (ST, SD, YT, and KT). Computed tomographic myelography findings were initially recorded by one reader (HE for cases 6 and 7 and by TO for case 8). The final interpretation of the CTM images was based on the consensus opinion of four authors (ST, SD, HE, and TO).

Similar low field MRI findings were obtained in cases 1–3. A large, left-sided mass extended dorsally from the affected disc space in the vertebral canal of all cases. The mass did not extend cranially or caudally. The mass caused a marked reduction in the diameter of the spinal cord of approximately 20–50%. The mass was hypointense, indicating an extruded calcified nucleus pulposus, in the T2-weighted images (T2WI) in all cases. Hyperintense lesions, indicating fluid, were observed on the left side, ventral to the spinal cord and proximally cranial and caudal to the mass in T2WI in all cases. The mass was hypointense in case 1 and slightly

hyperintense in case 3 in T1-weighted images (T1WI). The lesions indicating fluid were hypointense in T1WI in cases 1 and 3. The mass was described as mildly enhanced at the rim in postcontrast T1WI for case 3. Intervertebral disc herniations were suspected based on the MRI findings in these cases (Fig. 1). A secondary extradural hemorrhage was also suspected in case 3. For these cases, the surgical procedures were all conducted in the same manner. A left-sided hemilaminectomy was performed over the affected vertebral arch. No evidence of an epidural mass was found. Bluish regions were observed suggesting accumulation of cerebrospinal fluid in the subarachnoid space, through the dura mater, in all three cases. After a durotomy over this area (using a surgical microscope in cases 1 and 2), a large amount of cerebrospinal fluid was found to have leaked, and some intradural extramedullary crumbling white material with an irregular surface was observed. This material was gently removed with a microforceps and spinal cord pulsation was observed after their removal (Fig. 2). The incised dura mater was not closed.

Low field MRI findings were also similar for cases 4 and 5. A large, right-sided mass was observed in the vertebral canal dorsolateral to the spinal cord at the level of the affected intervertebral disc space. The mass did not extend cranially or caudally. The mass caused a marked reduction in the diameter of the spinal cord of approximately 50%. The mass was hypointense that suggested an extruded calcified nucleus pulposus in T2WI. In addition, a lesion with increased signal intensity was observed in both the gray and white matter of the spinal cord; this lesion extended from L2 to L3 in case 4 (Fig. 3). Dorsolateral intervertebral disc herniations were suspected in both cases, and secondary edematous cord changes were suspected in case 4 based on MRI findings. The surgical procedures were conducted in the same manner for both cases. A right-sided hemilaminectomy was performed over the affected vertebral arch. No evidence of an epidural mass was found. However, a focal spinal cord discoloration was observed at the intervertebral

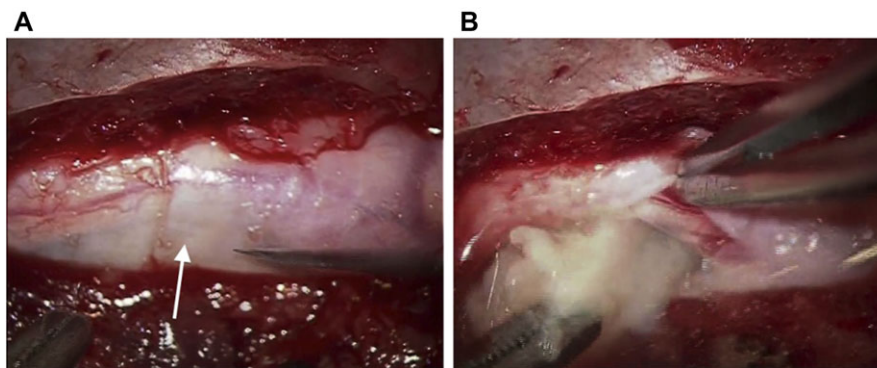


FIG. 2. Intraoperative photographs for case 1; (A) a bluish region (arrow) suggests an accumulation of cerebrospinal fluid through the dura mater over the L2–3 intervertebral disc space. (B) A large amount of cerebrospinal fluid had leaked after a durotomy and some crumbling white material was removed from the intradural extramedullary location.

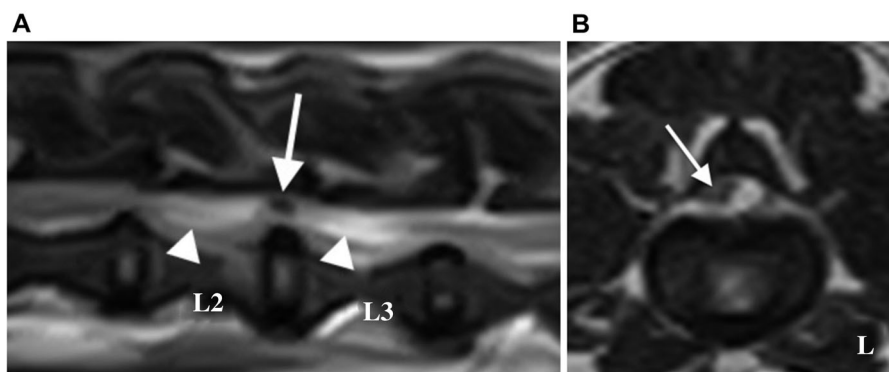


FIG. 3. Low field MRI scans for case 4. (A) T2-weighted right-sided parasagittal image. A hypointense mass (arrow) is observed at the level of the L2–3 intervertebral disc space. The spinal cord signal is increased (arrowheads) cranial and caudal to the level of the L2–3 intervertebral disc space over the length of two vertebral bodies. (B) T2-weighted transverse image. A hypointense mass is observed dorsolateral to the spinal cord (arrow). The spinal cord has increased signal intensity.

level (Fig. 4). During a careful palpation examination with a microprobe, the solid area was palpated at the center of the discolored area through the dura mater. After a durotomy of this area, a red region of the spinal cord was found in both cases. The region was focally soft to liquefy in case 4. A lateral linear myelotomy was performed over the abnormal spinal cord portion, and some crumbling white material with an irregular surface was removed with a microforceps from the spinal cord parenchyma. Spinal cord pulsation was observed after their removal. Incised dura mater was not closed.

With CTM, an intradural extramedullary lesion surrounded by an accumulation of contrast medium was observed in cases 6–8. This lesion compressed the spinal cord at the level of the intervertebral space. The filling deficit was relatively small in comparison to that predicted by the accumulation of contrast medium in common intradural extramedullary tumors, such as meningiomas or nerve sheath tumors. This imaging feature was more clearly described with multiplanar reconstruction dorsal images than axial

images. There was no evidence of contrast medium in the cord itself or any leaking into the extradural space (Fig. 5). Based on the acute onset and imaging findings, our main differential diagnosis was intervertebral disc extrusion that had penetrated the dura mater and compressed the spinal cord, causing a widening of the subarachnoid space. The same surgical procedure used for cases 1–3 was performed for cases 6–8, along with (cases 6, 7) and without (case 8) a surgical microscope.

All surgically removed materials, except those of cases 7 and 8, were identified as nucleus pulposus showing chondroid metaplasia upon histopathological examination;<sup>12</sup> no histopathological examination was performed for cases 7 and 8. Hemorrhage was observed in a removed nucleus pulposus sample from case 3. After making a diagnosis, we reviewed the MRI scans of cases 1–5. The hyperintense region in T2WI that we observed in cases 1–3, with an intradural extramedullary located nucleus pulposus, seemed to be the so-called “golf tee sign,” suggesting intradural extramedullary lesions (Fig. 6).

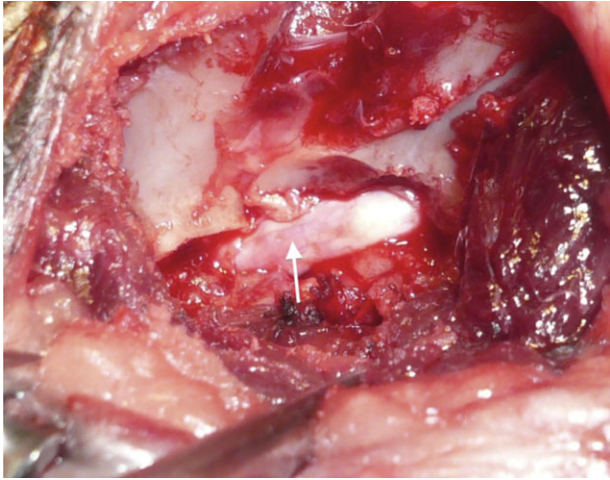


FIG. 4. Intraoperative photographs for case 4. A focal spinal cord discoloration (arrow) is observed through the dura mater over the L2–3 intervertebral disc space.

### Discussion

All cases in this study were relatively aged, and six of the eight cases had past histories of suspected intervertebral disc herniation. Seven of the eight cases were affected by intradural disc herniation between T11–12 and L2–3. These findings supported a previous pathophysiologic hypothesis developed for intradural disc herniation for humans.<sup>9,13</sup> Congenital and acquired adhesions involving the ventral dura mater, posterior (dorsal in dogs) longitudinal ligament, and annulus fibrosus have been proposed as predisposing factors. When adhesions among the dura, posterior longitudinal ligament, and annulus fibrosus occur, they can tear at the same time, causing nucleus pulposus dispersion into the subarachnoid space, resulting in intradural disc herniation.<sup>9,13</sup> Such adhesions and a lumbar intradural disc herniation occur at their highest frequency in the same location (L4–5 space) in humans.<sup>14</sup> Previous reports in dogs have indicated that more than 85% of intervertebral disc herniations occur between T11–12 and L2–3. Authors therefore hypothesize that intradural disc herniation in dogs of the current study may have occurred due to adhesions after a previous intervertebral disc herniation had resolved.<sup>15</sup>

Low field MRI studies did not identify clear, specific findings suggesting that the nucleus pulposus was in the subarachnoid space or in the spinal cord parenchyma for dogs of the current study. However, a limitation of this study was that MRI studies were not standardized and some were considered by readers to be insufficient. Not all studies included both T1WI and T2WI scans and postcontrast images. Conventional intervertebral disc herniation lesions have been described with various signal intensities and are often contrast enhanced in MRI studies because of secondary hemorrhage or inflammation and degeneration of the extruded

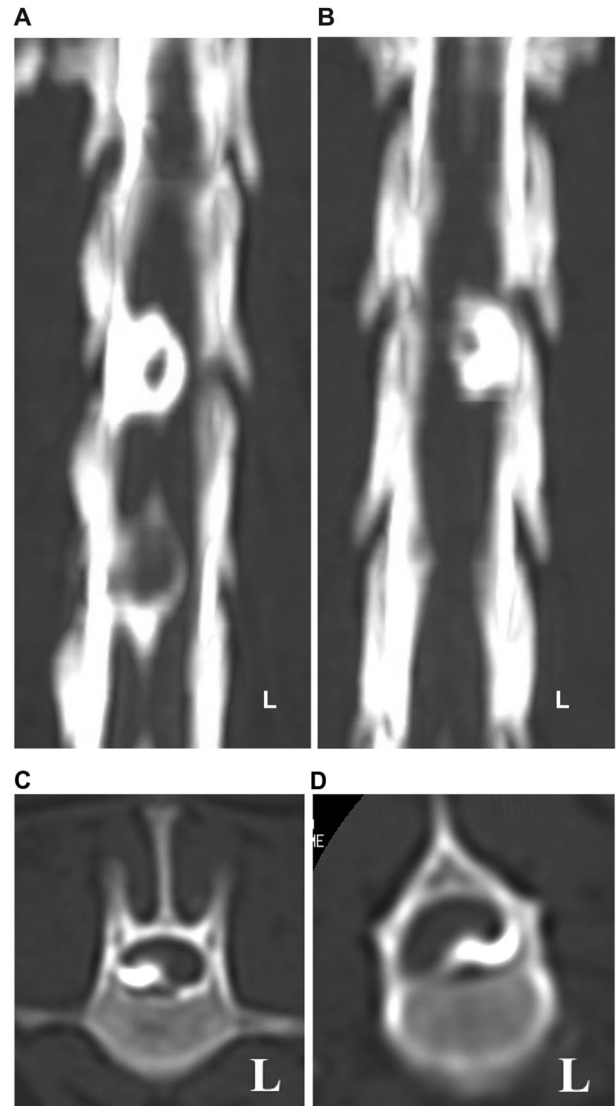


FIG. 5. Computed tomographic myelography (CTM) images generated using multiplanar reformatting. Dorsal planar and transverse planar views for cases 6 (A, C) and 7 (B, D) demonstrate a “golf tee sign” and filling deficit (arrows) at the level of the L1–2 (case 6) and T13–L1 (case 7) intervertebral disc space, respectively.

nucleus pulposus.<sup>16–19</sup> Retrospectively, readers for the current study reported that the T2WI hyperintense lesions seen in cases 1–3 seemed to be the “golf tee sign,” although this information was not available to surgeons before surgery. A “golf tee sign” can be theoretically differentiated from other conditions by using a combination of T2WI, T2\*WI, fluid-attenuated inversion recovery (FLAIR), and pre- and post-contrast T1WI,<sup>16–18</sup> as well as the single-shot turbo spin echo sequence or half-Fourier acquisition single-shot turbo spin-echo pulse sequence.<sup>20,21</sup> However, differentiation of these lesions using low-field MRI is not easy in the canine vertebral canal due to the smaller size vs. humans. The image spatial resolution and contrast in T2\*WI varies

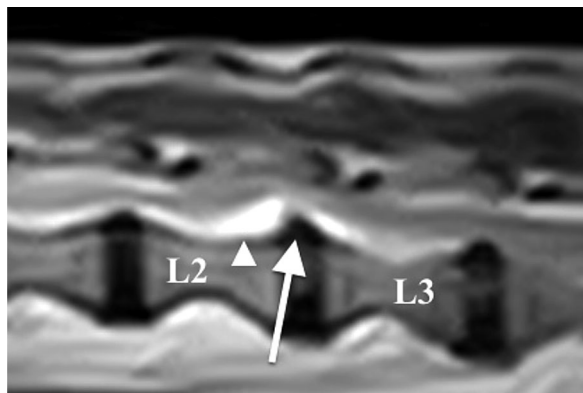


FIG. 6. Low field MRI scans for case 2. (A) T2-weighted left-sided parasagittal image. Hypointense (arrow) and hyperintense lesions indicating fluid (arrow heads) are observed at the level of the L2–3 intervertebral space. A “golf tee sign” suggesting an intradural extramedullary is evident.

with the field strength because of variations in signal-to-noise ratios.<sup>22,23</sup> For both intramedullary intradural disc herniation cases of the current study (cases 4, 5), there were no low field MRI findings suggesting penetration of the dura mater. Thus, all cases examined with low field MRI in the present report were preoperatively misdiagnosed as having conventional intervertebral disc herniation. This observation was consistent with previous reports in humans.<sup>10</sup> Intradural disc herniation may mimic the MRI findings of intradural extramedullary tumors, and the differentiation between these entities has been discussed for humans.<sup>24</sup> Authors recommend that intradural disc herniation be included in the differential diagnosis list for dogs with a suspected intradural extramedullary tumor based on MRI.

Previously reported standard myelography characteristics such as the “golf tee sign” and a subarachnoid filling deficit were observed with CTM in three of our cases.<sup>1,3,5,6</sup>

Authors propose that CTM may be more sensitive for detecting intradural disc herniation lesions than standard myelography in dogs due to the small size of the lesions. Intradural compression of the spinal cord with contrast medium accumulation and a circular filling defect has been previously reported in one canine case report of intradural disc herniation.<sup>7</sup> These findings have not been reported in conventional intervertebral disc herniations or canine spinal tumors. An extruded nucleus pulposus has an irregular surface without a capsule as would be expected in tumors. Contrast medium was distributed in the cleft of the nucleus pulposus in the subarachnoid space that had a smaller silhouette, visualized as a filling deficit with CTM. A human report have indicated that CTM is more valuable for demonstrating intradural disc herniations than MRI,<sup>25</sup> and another human report have declared that MRI is the most reliable method for diagnosis of intradural disc herniation.<sup>14</sup> Authors of the current study propose that the chance of finding small lesions in a limited anatomic location may be greater with CTM than with low-field MRI in dogs, because CT units have a smaller voxel size than the low-field MRIs used here.

In conclusion, prevalence findings from this study supported previous reports indicating that canine thoracolumbar intradural disc herniation is a rare condition. Observations such as the “golf tee sign” and a filling deficit (which was relatively small compared to the contrast medium accumulation on CTM) were indicators of an intradural extramedullary disc herniation for some of the dogs. Based on this small sample of eight dogs, authors propose that CTM may be more valuable for demonstrating canine intradural disc herniation than low-field MRI. Future controlled studies are needed to compare diagnostic sensitivities of low-field MRI, high-field MRI, and CTM for detecting canine intradural disc herniation.

APPENDIX 1. Clinical and Imaging Characteristics of eight Dogs with Confirmed Thoracolumbar Intradural Disc Herniation

No.	Breed	Age (Years)	History	Lesion	MRI* magnet strength/sequence	MRI findings	CTM† findings	Nucleus
1	Miniature Dachshund	11	+	L2–3	0.3T/T2WI‡: SAG, TRS, T1WI§: TRS	NS <sup>  </sup> (GTS¶)	NE <sup>#</sup>	ID/EM**
2	Miniature Dachshund	10	+	L2–3	0.3T/T2WI: SAG, TRS	NS <sup>  </sup> (GTS¶)	NE	ID/EM
3	Miniature Dachshund	12	+	L3–4	0.2T/T2WI: SAG, TRS, pre- and post-contrast T1WI: SAG, TRS	NS <sup>  </sup> (GTS¶)	NE	ID/EM
4	Miniature Dachshund	7	+	L2–3	0.3T/T2WI: SAG, TRS, DOR	NS	NE	IM***
5	mixed small dog	13	+	L2–3	0.3T/T2WI: SAG, TRS	NS	NE	IM
6	Maltese	13	–	L1–2	NE	NE	An intradural extramedullary lesion surrounded by accumulated contrast medium	ID/EM
7	Chihuahua	9	–	T13-L1	NE	NE	An intradural extramedullary lesion surrounded by accumulated contrast medium	ID/EM
8	Miniature Dachshund	9	+	L2–3	NE	NE	an intradural extramedullary lesion surrounded by accumulated contrast medium	ID/EM

History: suspected intervertebral disc herniation such as prior back pain or paraparesis

\*MRI, Magnetic resonance imaging.

†CTM, computed tomographic myelography.

‡T2WI, T2-weighted images.

§T1WI, T1-weighted images.

||NS, nonspecific to intradural intervertebral disc herniation and could not be differentiated from conventional intervertebral disc herniation.

¶GTS, Golf tee sign, but difficult to differentiate from conventional intervertebral disc herniation.

#NE, not examined.

\*\*ID/EM, intradural extramedullary.

\*\*\*IM, intramedullary.

## REFERENCES

- Packer RA, Frank PM, Chambers JN. Traumatic subarachnoid-pleural fistula in a dog. *Vet Radiol Ultrasound* 2004;45:523–527.
- Sanders SG, Bagley RS, Gavin PR. Intramedullary spinal cord damage associated with intervertebral disk material in a dog. *J Am Vet Med Assoc* 2002;221:1594–1596.
- Liptak JM, Allan GS, Krockenberger MB, Davis PE, Malik R. Radiographic diagnosis: intramedullary extrusion of an intervertebral disk. *Vet Radiol Ultrasound* 2002;43:272–274.
- Poncelet L, Heimann M. Intradural lumbar disk herniation in a dog. *Vet Rec* 2011;168:486a.
- Roush JK, Douglass JP, Hertzke D, Kennedy GA. Traumatic dural laceration in a racing greyhound. *Vet Radiol Ultrasound* 1992;33:22–24.
- Montavon PM, Weber U, Guscetti F, Suter PF. What is your diagnosis? Swelling of spinal cord associated with dural tear between segments T13 and L1. *J Am Vet Med Assoc* 1990;196:783–784.
- Barnoon I, Chai O, Srugo I, Peeri D, Konstantin L, Brenner O, et al. Spontaneous intradural disc herniation with focal distension of the subarachnoid space in a dog. *Can Vet J* 2012;53:1191–1194.
- Kent M, Holmes S, Cohen E, Sakals S, Roach W, Platt S, et al. Imaging diagnosis-CT myelography in a dog with intramedullary intervertebral disc herniation. *Vet Radiol Ultrasound* 2011;52:185–187.
- Ozturk A, Avci E, Yazgan P, Torun F, Yucetas S, Karabag H. Intradural herniation of intervertebral disk at the level of lumbar 1–lumbar 2. *Turk Neurosurg* 2007;17:134–137.
- D'Andrea G, Trillo G, Roperto R, Celli P, Orlando ER, Ferrante L. Intradural lumbar disc herniations: the role of MRI in preoperative diagnosis and review of the literature. *Neurosurg Rev* 2004;27:75–80.
- McConnell JF, Garosi LS. Intramedullary intervertebral disk extrusion in a cat. *Vet Radiol Ultrasound* 2004;45:327–330.
- Royal AB, Chigerwe M, Coates JR, Wiedmeyer CE, Berent LM. Cytologic and histopathologic evaluation of extruded canine degenerate disks. *Vet Surg* 2009;38:798–802.
- Yildizhan A, Pasaoglu A, Okten T, Ekinci N, Aycan K, Aral O. Intradural disk herniations pathogenesis, clinical picture, diagnosis and treatment. *Acta Neurochir (Wien)*. 1991;110:160–165.

14. Arnold PM, Wakwaya YT. Intradural disk herniation at L1-L2: report of two cases. *J Spinal Cord Med* 2011;34:312-314.
15. Sharp NJH, Wheeler SJ. Thoracolumbar disc disease. In: *Small animal spinal disorders diagnosis and surgery*, 2nd ed. Philadelphia: Mosby, 2005;121-160.
16. Tidwell AS, Specht A, Blaeser L, Kent M. Magnetic resonance imaging features of extradural hematomas associated with inter vertebral disk herniation in a dog. *Vet Radiol Ultrasound* 2002;43:319-324.
17. Mateo I, Lorenzo V, Foradada L, Munoz A. Clinical, pathological, and magnetic resonance imaging characteristic of canine disc extrusion accompanied by epidural hemorrhage or inflammation. *Vet Radiol Ultrasound* 2011;52:17-24.
18. Sether LA, Nguyen C, Yu SN, Haughton VM, Ho KC, Biller DS, et al. Canine intervertebral disk: correlation of anatomy and MR imaging. *Radiology* 1990;175:207-211.
19. Suran JN, Durham A, Mai W, Seiler GS. Contrast enhancement of extradural compressive material on magnetic resonance imaging. *Vet Radiol Ultrasound* 2011;52:10-16.
20. Pease A, Sullivan S, Olby N, Galano H, Cerda-Gonzalez S, Robertson ID, et al. Value of a single-shot turbo spin-echo pulse sequence for assessing the architecture of the subarachnoid space and the constitutive nature of cerebrospinal fluid. *Vet Radiol Ultrasound* 2006;47:254-259.
21. Sellar GS, Robertson ID, Mai W, Widmer WR, Suran J, Nemanic S, et al. Usefulness of a half-fourier acquisition single-shot turbo spin-echo pulse sequence in identifying arachnoid diverticula in dogs. *Vet Radiol Ultrasound* 2012;53:157-161.
22. Luyypaert R, Goes E, Osteaux M. MRI tissue differentiation: comparing high and low field strength. *J Belge Radiol* 1986;69:157-161.
23. Nandigam RN, Viswanathan A, Delgado P, Skehan ME, Smith EE, Rosand J, et al. MR imaging detection of cerebral microbleeds: effect of susceptibility-weighted imaging, section thickness, and field strength. *AJNR Am J Neuroradiol* 2009;30:338-343.
24. Liu CC, Huang CT, Lin CM, Liu KN. Intradural disk herniation at L5 level mimicking an intradural spinal tumor. *Eur Spine J* 2011;20(Suppl 2):S326-S329.
25. Epstein NE, Syrquin MS, Epstein JA, Decker RE. Intradural disc herniations in the cervical, thoracic, and lumbar spine: report of three cases and review of the literature. *J Spinal Disord* 1990;3:396-403.